

Energy-Autonomous Roadside Nodes in V2I Using RF Energy Harvesting

JOSE MANUEL GIMENEZ-GUZMAN¹, ISRAEL LEYVA-MAYORGA² (Member, IEEE),
AMIRHOSSEIN AZARBAHRAM³ (Graduate Student Member, IEEE),
ONEL ALCARAZ LÓPEZ³ (Senior Member, IEEE), AND PETAR POPOVSKI² (Fellow, IEEE)

¹Department of Communications, Universitat Politècnica de València, 46022 Valencia, Spain

²Department of Electronic Systems, Aalborg University, 9220 Aalborg, Denmark

³Centre for Wireless Communications, University of Oulu, 90014 Oulu, Finland

CORRESPONDING AUTHOR: J. M. GIMENEZ-GUZMAN (e-mail: jmgimenez@upv.es)

This work was supported in part by the MCIN/AEI/10.13039/501100011033 and the European Union "NextGenerationEU"/PRTR under Project TED2021-131387B-I00; in part by the MCIN/AEI/10.13039/501100011033/FEDER, UE under Project PID2021-123168NB-I00; in part by the Villum Investigator Grant "WATER" from the Velux Foundation, Denmark; in part by the Finnish Foundation for Technology Promotion; and in part by the Research Council of Finland (former Academy of Finland) under Grant 348515 and Grant 346208 (6G Flagship Programme).

ABSTRACT Future intelligent transportation systems will require complex networking infrastructures with communication among a huge number of vehicles and roadside nodes to support services such as autonomous driving. However, the deployment and operation of such a large number of roadside nodes is expensive due to either the cost of battery replacement or the maintenance of a continuous energy supply in long highways or rural areas. In this work, we evaluate the feasibility of a roadside unit harvesting energy from radio frequency (RF) signals transmitted by a nearby moving vehicle, with the incentive of using a part of the harvested energy to transmit small amounts of data to the vehicle. We consider a realistic model with the timing elements related to the movement of the vehicle, beam tracking errors, a non-linear model for energy harvesting, and potential line-of-sight obstructions in multi-vehicle scenarios. Results show that, with typical off-the-shelf components, it is feasible to use the RF harvested energy to transmit between a few hundred and several thousand bytes, depending on the speed of vehicles and the frequency of operation for energy harvesting, among other parameters.

INDEX TERMS Intelligent transportation systems, RF energy harvesting, V2I communications.

I. INTRODUCTION

FUTURE Intelligent Transportation Systems (ITS) will radically transform human mobility by offering a plethora of new transportation services that will increase safety, comfort, and efficiency. These services include platooning, advanced driving, remote driving, and extended sensing, which may ultimately enable autonomous driving [1], [2]. To support these services, ITS are based on an underlying complex data network infrastructure, shaping the so-called Vehicle-to-Everything (V2X) networks. Note that V2X agglutinates several possible interlocutors for vehicles, ranging from another vehicle (V2V), a pedestrian (V2P), the cloud network (V2N), or the infrastructure (V2I).

ITS are often associated with the smart cities of the future [3]. However, to avoid widening the development gap between urban and rural areas and to provide service continuity over large areas, it is crucial that ITS services like autonomous driving are also accessible in rural regions. Achieving this goal might require the deployment of an extremely large number of roadside nodes, which can broadcast safety warnings or indications for driving to passing vehicles to improve the safety and efficiency of mobility or even perform tasks related to the authentication of vehicles and roadside nodes to strengthen security [4]. One of the biggest concerns when deploying infrastructure nodes is related to their energy source, which can stem from either batteries or directly from the electric grid. Nevertheless,

access to a reliable power supply in rural areas is not guaranteed. If the roadside nodes are powered by the electric grid, downtimes may be significantly low depending on the grid's reliability, but deploying a power grid infrastructure to support the deployment of roadside nodes would incur prohibitive deployment and/or maintenance costs, oftentimes exceeding the cost of the roadside nodes themselves. On the other hand, if the nodes are equipped with batteries, OPEX (Operational EXpenses) may be high due to the need for frequent human intervention to recharge, repair, or change batteries, in addition to its non-negligible initial cost [5].

In recent years, the research community has paid more attention to energy efficiency in wireless networking, initiating the so-called green networking era [6]. Future ITS, which will be supported by the sixth generation (6G) communication technology, will require massive densely deployed network infrastructures consuming extremely high amounts of energy. Therefore, to make ITS applications viable, it is mandatory to minimize the deployment and maintenance costs of roadside infrastructure nodes. In this regard, energy harvesting (EH) [7] has emerged as a key technique to collect energy from the environment, which can be used to minimize the reliance of the nodes on battery replacement campaigns. The main EH sources include solar radiation, wind, structural vibrations, heat, and radio frequency (RF) signals. It is also possible to perform EH from multiple sources to increase the total amount of harvested energy, as well as the harvesting continuity, to increase the reliability of the EH systems. For example, relying only on EH from solar radiation may not be efficient due to its unpredictability and, hence, energy can be harvested from other sources such as RF signals. A detailed description and evaluation of the pros and cons of different EH sources can be found in [8].

In this paper, we carry out a feasibility and performance analysis for the use of energy-autonomous roadside nodes that harvest energy from the RF signals of nearby vehicles to send data back to these vehicles. The main hypothesis of this work is that current off-the-shelf technologies for RF EH and communications can be used to ease the deployment of roadside nodes by avoiding the replacement of batteries and the need for a connection to the electric grid. The main contributions of our work are the following.

- We propose a realistic system model that jointly considers an RF EH nonlinear model and a wireless communication model for the scenarios with a moving vehicle equipped with a planar antenna array for energy beamforming. Our model considers the timing aspects due to the vehicle movement using realistic models for beam tracking errors and potential line-of-sight obstructions.
- We analyze the impact of the speed of the vehicles on the amount of energy that can be harvested and the amount of data that roadside nodes can transmit when using only energy harvested from RF signals.

TABLE 1. Main notations used in the paper.

Notation	Definition
T	Frame length
$\alpha_{\text{WET}}/\alpha_{\text{WIT}}$	Time fraction of WET/WIT stages
P_{rc}^{WPN}	Operation power of WPN
$E_h/P_h/P_h^{\text{max}}$	Harvested energy/power/maximum power by the WPN
$P_{tr,x}^v/P_{tr,x}^{\text{WPN}}$	Vehicle/WPN transmission power
$P_{lc}^{\text{WPN}}/P_{lc}^{\text{WPN}}$	Power required/consumed by WPN to transmit data
P_{rx}	Received power at WPN
σ/ζ	Parameters of EH circuit
$M \times N$	URPA size at vehicles
$a(\theta, \phi)$	URPA steering vector at azimuth/elevation angles
δ	Space between URPA elements
$\lambda_{\text{WET}}/\lambda_{\text{WIT}}$	Wavelength of WET/WIT signals
$\mathbf{w}(t)$	URPA digital precoding vector
F_M/F_N	Factor to represent URPA radiation pattern
BTE	URPA beam tracking error
$v_s/v_\perp/\omega$	Vehicle speed/cross-radial speed/angular speed
d/r	Distance/minimum distance from vehicle to WPN
ℓ	Path loss exponent
K_0	Friis equation parameter
$\mathbf{h}(t)$	Channel gain
P_{NLoS}	Probability of obstruction of the LoS
G_v/G_{WPN}	Vehicle/WPN antenna gain
L	Packet length
R	Data transmission rate
Δ	Extra fraction of energy harvested by WPN
E_c	Energy consumed by WPN
$E_{tr,x}^{\text{WPN}}/T_{tr,x}$	Energy/time required by WPN to send a packet
s_m	Minimum separation of vehicles for safety
s	Separation of adjacent vehicles
Λ	Density of vehicles

- We propose and evaluate a setting with multiple vehicles transmitting energy to the roadside infrastructure to analyze how the performance changes with respect to the single-vehicle setting.

The paper is structured as follows. In Section II, we identify and describe other related works in the literature, while in Section III, we describe the scenario under study and the two main stages, namely wireless energy transfer and wireless information transfer. In Sections IV and V we describe the realistic models used for both stages and for the multi-vehicle evaluation, respectively. Finally, in Section VI, we show the main results of this study while in Section VII, we conclude the paper by summarizing the main results and shedding light on future research directions in the area of EH-enabled ITS.

To ease readability, all the main notations of the paper are summarized in Table 1.

II. RELATED WORK

A. ENERGY HARVESTING IN ITS

The development of energy-efficient ITS has attracted the attention of researchers because of its importance for our

current society [9]. In [10], the authors study energy efficiency in V2X networks from a holistic point of view as they consider EH, communications, computation, traffic management, and electric vehicles (EV), including energy consumption discussions. A large portion of the EH-related literature [10] focuses on the use of renewable energy sources. For example, in [11], [12], [13], the authors propose to use wind or solar-powered roadside units to avoid its connection to the smart grid. Other studies, e.g., [14], propose using the vibrational energy induced by vehicles moving. Notwithstanding, the possibility of harvesting energy from several sources simultaneously has also been considered [15]. In [16], it is proposed a setting that uses both EH from renewable sources and RF EH. More specifically, it proposes a collaborative energy management scheme that, instead of avoiding the use of batteries or connection to the electric grid, considers the possibility of selling redundant energy between roadside units and EVs (in both directions).

B. RF ENERGY HARVESTING FOR COMMUNICATIONS

The proposal of performing energy transfer and information transmission as a two-stage procedure has already appeared in the literature in several contexts [17], [18], [19], [20], [21], [22]. For example, an interesting work related to ours is [17], where the authors consider a cognitive radio network for connected vehicles where secondary users (vehicles) can perform RF EH in the downlink and then send data in the uplink using the harvested energy. Although not in the field of terrestrial vehicular networking but in unmanned aerial vehicle (UAV), the authors in [18] propose transferring energy from UAV to users while users use that harvested energy for data transmission to the UAV or even for federated learning [19]. Moreover, a scheme where multiple sources harvest energy from a dedicated power station and communicate with a receiving station is proposed in [20], and for a single access point instead of multiple sources in [21]. Finally, in [22], the authors use wireless energy transfer followed by an information transfer stage while studying the role of massive antenna systems for this type of deployment. These two-stage procedures are similar to the one we present in this paper, but neither are focused on a V2I setting nor explore the limits of data transmission, as our work does. Similar to the above-described papers, it is worth referring to [23], [24], [25], [26], where there is also a two-stage procedure but wireless power transfer is used for mobile edge computing instead of communication purposes.

As stated in Section I, in this paper we focus on exploiting RF EH to deploy energy-autonomous network nodes. This perspective is quite innovative as usually RF EH is oriented to alleviate energy consumption instead of being the only energy source. For example, a deep learning-based resource allocation procedure using EH to aid V2X communications is proposed in [27], but harvested energy is not the only energy source. Another example is [16], wherein the authors propose a collaborative energy management scheme that, instead of avoiding the use of

batteries or connection to the electric grid, considers the possibility of selling redundant energy between roadside units and EV (in both directions). Notwithstanding, there have been some proposals that propound energy autonomous network nodes, being [28], [29], [30] some of the most outstanding works in this research field. For example, [30] proposes the use of multiple frequency bands to improve the EH procedure. In the area of zero-energy devices, it is important to highlight [28], where the authors thoroughly study the problem of powering massive Internet of Things (IoT) networks using RF EH. As we can see, there have been some recent efforts to have energy-autonomous nodes in IoT environments. However, to the best of our knowledge, the only work that considers RF EH in a vehicular environment to power a harvesting device is [31], which emphasizes that using RF EH in vehicular communications is yet an unexplored research direction. More specifically, the authors analyze a setting where moving vehicles charge with RF signals a device alongside the road, which later transmits information to an access point. Despite these similarities, our work includes several aspects not considered in [31], with some of them being listed as future work. These aspects include considering variable vehicle speeds and time-varying inter-vehicle distances, a non-linear model for RF EH, and a realistic model for beamforming at the vehicles with imperfect steering.

Finally, surveying the related work in the area of RF-powered networks is not complete without referring to the main efforts related to performing data transmission simultaneously with energy transfer. This possibility, called Simultaneous Wireless Information and Power Transfer (SWIPT), has gained the attention of the scientific community during the last years, where we can highlight the works [32], [33], [34], [35]. For instance, a device-to-device communication framework is proposed in [35] for SWIPT IoT systems. However, SWIPT has also been considered specifically for vehicular environments. For example, in [36], the authors study SWIPT in V2X environments, considering that vehicles are able to collect energy from the RF signals transmitted by a base station.

In Table 2, we summarize the main features of the scenarios considered in the literature that are more relevant to our work. Note that the types *dynamic* and *static* represent the situation when it is considered the motion of the node that transmits or receives energy signals or not, respectively.

III. ENERGY-AUTONOMOUS NODES IN V2I

We consider a road with a wireless-powered roadside node (WPN) on the sidewalk and a vehicle that drives across that road, as shown in Fig. 1. To make the operation of such WPN feasible, the vehicle must rely on passive detection mechanisms, from the WPN perspective, such as object detection with cameras. Otherwise, WPNs can be also geolocalized as their localization can be easily gathered from other nearby WPN or even from the Internet. The objective of the WPN is to send data to vehicles making

TABLE 2. Summary table of features of the scenario considered in the literature and in the current paper.

Reference	Setting	Type	RF EH device	Energy-autonomous nodes	Harvest-then-transmit	Non-linear EH model	Antenna array
[17]	V2X	Static	Vehicle	✓	✓		
[18]	UAV	Dynamic	Generic	✓	✓		✓
[20]	Generic	Static	Generic	✓	✓		
[21]	Relay	Static	Access point	✓	✓	✓	✓
[22]	Generic	Static	Generic	✓	✓	✓	✓
[31]	V2X	Dynamic	Roadside unit	✓	✓		
[36]	V2X	Static	Vehicle			✓	✓
Current paper	V2X	Dynamic	Roadside unit	✓	✓	✓	✓

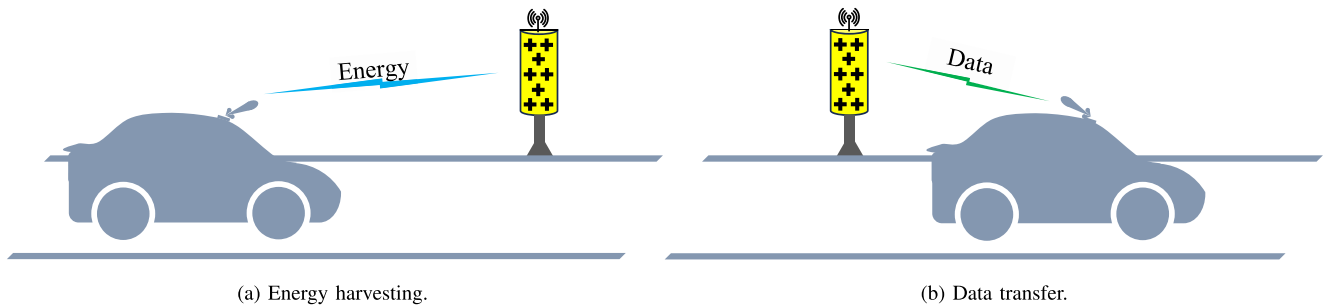


FIGURE 1. Setting under study.

use only of the energy previously harvested from the RF transmissions of that vehicle. Depending on the purpose of the WPN, this information can be diverse. A representative and meaningful example could be a WPN that transmits information about traffic restrictions (like maximum speed) or potential hazards to autonomous vehicles. It is important to note that this information is pre-defined or can come (whenever there is enough energy to receive data) from a core network periodically. In general, the information to transmit can depend on several parameters such as time of the day, day of the week, month, or weather conditions, among many others. For example, near a school, the WPN can transmit a more restricted speed limit to autonomous vehicles during the weekdays at the times when children enter or leave school or when the weather conditions are adverse.

The aforementioned system operates in a Time Division Duplex (TDD) mode with two stages. The first one is a Wireless Energy Transfer (WET) phase from the vehicle to the WPN, while the second one consists of a Wireless Information Transfer (WIT) stage from the WPN to the vehicle. The consecutive operation of both stages, illustrated in Fig. 2, constitutes a frame, whose length is T , being the time fraction of WET and WIT stages α_{WET} and α_{WIT} , respectively. Note that, under this setting, $\alpha_{\text{WET}} + \alpha_{\text{WIT}} = 1$, while T is bounded by the time the vehicle remains in the coverage area of the WPN.

The energy consumption during the whole operation for serving a vehicle can be computed as the sum of the energy consumed in the WET stage and the one consumed in the WIT stage. During the WET stage, WPN is in reception

mode, so it only consumes the energy required to power the receiving circuit, being this power P_{rc}^{WPN} . Note that we do not consider information transmission to the WPN to avoid the energy-consuming procedure due to the decoding procedure. Then, the energy consumption by the WPN during the WET stage can be computed by $P_{rc}^{\text{WPN}} \alpha_{\text{WET}} T$.

Let E_h be the energy harvested by the WPN, thus $E_h - P_{rc}^{\text{WPN}} \alpha_{\text{WET}} T > 0$ must hold to support the EH process. In the case $E_h - P_{rc}^{\text{WPN}} \alpha_{\text{WET}} T \leq 0$, the EH process is not successful. The latter can be due to a very low channel gain, a low transmission power from the vehicle, a low energy conversion efficiency, or a large circuit power consumption. To transmit the information from WPN to the vehicle as soon as possible, we propose a “harvest-then-transmit” strategy, originally proposed in [37]. In the next section, we describe the wireless EH model and the wireless information transfer model in detail.

IV. SYSTEM MODEL

To model WET procedure, we assume that vehicles know the position of WPNs, as WPNs can be detected by making use of object detection computer vision techniques already available in vehicles, complemented with geolocation information gathered from other near WPN or from the Internet. From that information, when the vehicle is close to a WPN it can start with the WET stage by wireless powering that WPN. More specifically, the vehicle broadcasts an energy RF signal using a transmission power P_{trx}^v , while the WPN makes use of a “harvest-then-transmit” strategy. The use of this strategy allows to reduce the device cost

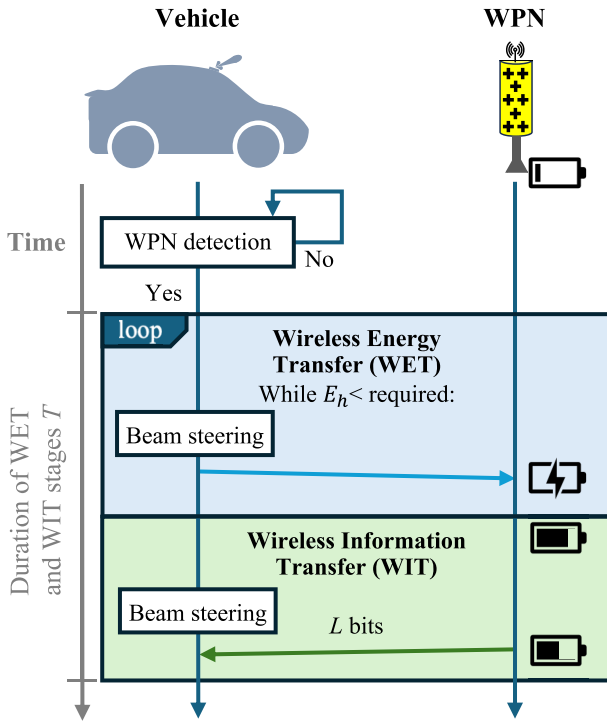


FIGURE 2. Time diagram with the TDD operation of the system. The WET stage begins when a WPN node is detected and ends when it has harvested sufficient energy for data transmission.

compared to other strategies that require large and costly batteries. In other words, the harvested energy is put to be used for transmission as long as there is enough available energy.

To account for the amount of harvested power that the WPN can obtain from the signal transmitted by the vehicle, we consider that the harvested power $P_h(t)$ is a nonlinear function of the input power $P_{rx}(t)$, which is the received power signal from the vehicle. In more detail, we use a curvilinear EH model based on the logistic (sigmoidal) function to capture the nonlinearity behavior due to hardware constraints such as sensitivity limitations and current leakage. Basically, due to the saturation of harvesting circuits, the maximum harvested power is upper bounded to a value of P_h^{\max} . With that, the harvested power can be computed as [33]:

$$P_h(P_{rx}(t)) = \frac{P_h^{\max} \left(\frac{1}{1+e^{-\sigma(P_{rx}(t)-\zeta)}} - \frac{1}{1+e^{\sigma\zeta}} \right)}{1 - \frac{1}{1+e^{\sigma\zeta}}}, \quad (1)$$

where σ and ζ are constant values that depend on parameters of the EH circuit such as the capacitance or diode turn-on voltage.

We consider that each vehicle is equipped with a uniform rectangular planar array (URPA) that uses digital beamforming to maximize the amount of energy available for harvesting at the WPN. The URPA consists of an array of

$M \times N$ antennas such that the array steering vector for an azimuth angle θ and elevation angle ϕ equals to [38]:

$$\mathbf{a}(\theta, \phi) = \frac{1}{\sqrt{MN}} \left[1, \dots, e^{jk\delta \sin \phi [(m-1) \cos \theta + (n-1) \sin \theta]}, \dots, e^{jk\delta \sin \phi [(M-1) \cos \theta + (N-1) \sin \theta]} \right]^T, \quad (2)$$

where $0 \leq m \leq M$ and $0 \leq n \leq N$ and being δ the spacing between elements, k the wavenumber, i.e., $k = 2\pi/\lambda_{\text{WET}}$ and $\iota = \sqrt{-1}$ denotes the imaginary unit.

For a more convenient representation, it is possible to make the following coordinate transformation:

$$\Upsilon = \sin \phi \cos \theta, \quad (3)$$

$$\Psi = \sin \phi \sin \theta, \quad (4)$$

Then, (2) can be rewritten as:

$$\mathbf{a}(\Upsilon, \Psi) = \frac{1}{\sqrt{MN}} \left(\left[1, \dots, e^{jk\delta(M-1)\Upsilon} \right]^T \otimes \left[1, \dots, e^{jk\delta(N-1)\Psi} \right]^T \right), \quad (5)$$

where \otimes denotes the Kronecker product. Note that using (5) the beam pattern can be designed at the directions Υ and Ψ independently.

For a half-wavelength-URPA, where $\delta = \lambda_{\text{WET}}/2$, (5) becomes:

$$\mathbf{a}(\Upsilon, \Psi) = \frac{1}{\sqrt{MN}} \left(\left[1, \dots, e^{j\pi(M-1)\Upsilon} \right]^T \otimes \left[1, \dots, e^{j\pi(N-1)\Psi} \right]^T \right). \quad (6)$$

Then, the vehicle chooses a direction (Υ_b, Ψ_b) aiming at the WPN and transmits the beam \mathbf{b} :

$$\mathbf{b} = \mathbf{a}(\Upsilon_b, \Psi_b). \quad (7)$$

The choice of (Υ_b, Ψ_b) is guided by the goal of digital beamforming, which is equivalent to maximizing the harvested power at the WPN by aligning the main lobe of the URPA with the direction between the vehicle and the WPN. Defining $\mathbf{w}(t)$ as the dedicated $M \times N$ -dimensional digital precoding vector for the energy symbol at time t , the problem of maximizing the harvested energy at the WPN can be formally stated as:

$$\max_{\mathbf{w}(t)} P_h(P_{rx}(t)) \quad (8a)$$

$$\text{s.t. } |\mathbf{w}(t)|^2 \leq P_{tx}^{\max}. \quad (8b)$$

Furthermore, it is evident from (1) that the optimization objective $P_h(P_{rx}(t))$ is monotonically increasing with the received power and, hence, $P_h(P_1) \leq P_h(P_2)$ for all $P_1 \leq P_2$ and, naturally, $\lim_{P_{rx}(t) \rightarrow \infty} P_h(P_{rx}(t)) = P_h^{\max}$. Therefore, we can write the equivalent problem as

$$\max_{\mathbf{w}(t)} P_{rx}(t). \quad (9a)$$

$$\text{s.t. } |\mathbf{w}(t)|^2 \leq P_{tx}^{\max}. \quad (9b)$$

It has been proven that the optimal precoders for (9) can be obtained by applying maximum ratio transmission (MRT) [39], which gives $\mathbf{w}^*(t) = \frac{\mathbf{h}(t)}{|\mathbf{h}(t)|} \sqrt{P_{tx}^{\max}}$, with $\mathbf{h}(t) = [h_1(t), \dots, h_{M \times N}(t)]^T$ being the concatenated channel vector between the WPN and the antenna array at time t .

Although the objective is to maximize the harvested energy, in this work we are also interested in investigating the effect on the harvested energy when the beam is not perfectly aligned in the direction where the WPN is located. More specifically, and considering that the elements of the URPA radiate isotropically, the beam pattern of the vehicle antenna for a direction $(\bar{\mathcal{U}}, \Psi)$ when the beam is aimed at direction $(\bar{\mathcal{U}}_b, \Psi_b)$ can be expressed as:

$$G_v(\bar{\mathcal{U}}, \Psi, \bar{\mathcal{U}}_b, \Psi_b) = MN F_M(\bar{\mathcal{U}}, \bar{\mathcal{U}}_b) F_N(\Psi, \Psi_b), \quad (10)$$

where $F_M(\bar{\mathcal{U}}, \bar{\mathcal{U}}_b)$ represents a factor in the range $[0, 1]$ to represent the radiation pattern for different directions of $\bar{\mathcal{U}}$ with respect to its maximum gain, that is produced in the direction of the beam $\bar{\mathcal{U}}_b$. Note that $F_N(\Psi_b, \Psi)$ is the equivalent factor for direction Ψ . When the beam is perfectly aligned with the direction of the location of the WPN, $F_M(\bar{\mathcal{U}}, \bar{\mathcal{U}}_b) F_N(\Psi, \Psi_b) = 1$. Note also that $F_M(\bar{\mathcal{U}}, \bar{\mathcal{U}}_b)$ and $F_N(\Psi, \Psi_b) = 1$ can be expressed as a function of the Fejér kernel of order M and N respectively, being $F_M(\cdot)$ and $F_N(\cdot)$. More specifically,

$$F_M(\bar{\mathcal{U}}, \bar{\mathcal{U}}_b) = \frac{F_M(\bar{\mathcal{U}} - \bar{\mathcal{U}}_b)}{M}, \quad (11)$$

$$F_N(\Psi, \Psi_b) = \frac{F_N(\Psi - \Psi_b)}{N}, \quad (12)$$

with

$$F_M(\bar{\mathcal{U}} - \bar{\mathcal{U}}_b) = \frac{\sin^2\left(\frac{\pi(\bar{\mathcal{U}} - \bar{\mathcal{U}}_b)M}{2}\right)}{M \sin^2\left(\frac{\pi(\bar{\mathcal{U}} - \bar{\mathcal{U}}_b)}{2}\right)}, \quad (13)$$

$$F_N(\Psi - \Psi_b) = \frac{\sin^2\left(\frac{\pi(\Psi - \Psi_b)N}{2}\right)}{N \sin^2\left(\frac{\pi(\Psi - \Psi_b)}{2}\right)}. \quad (14)$$

Finally, it is known that the beam tracking error (BTE), defined as the angular difference between the direction of the beam and the direction of the WPN, is higher with the angular velocity (ω) [40], so we have considered that $\text{BTE} = \xi \omega$ for both azimuth and elevation angles, where BTE is expressed in degrees and ξ is a factor that represents the accuracy of the beam tracking technique. Note that the BTE includes the effect of inaccuracies in the detection of the position of the WPN. Then, to compute BTE we must first calculate the angular velocity of the vehicle regarding the WPN (ω). Being φ the angle in the azimuth between the direction of the movement of the vehicle and the direction between the vehicle and the WPN, ω can be computed as:

$$\omega = \frac{d\varphi}{dt} = \frac{v_{\perp}}{d}, \quad (15)$$

where v_{\perp} is the cross-radial speed of the vehicle, which can be computed in terms of the vehicle speed across the

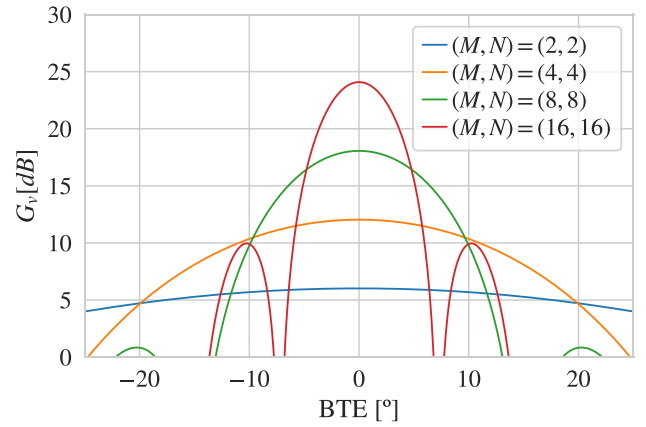


FIGURE 3. Vehicle antenna gain as a function of the beam tracking error for different antenna sizes.

road (v_s) as $v_{\perp} = v_s \sin \varphi$. Moreover, being r the minimum distance between the vehicle and the WPN (when the vehicle driving by the road passes the WPN), angle φ can be computed as:

$$\varphi = \arctan \frac{r}{d}. \quad (16)$$

To ease the understanding of the performance of the URPA, we show in Fig. 3 how vehicle antenna gain changes with the BTE for different antenna array sizes. As we can conclude from the figure, the beam width of the main lobe decreases as the number of antenna elements increases, resulting in a higher gain but also in a higher sensitivity to beam alignment errors.

On the other hand, for the channel between the vehicle and the WPN, we consider an additive white Gaussian noise (AWGN) channel with line of sight (LoS), where the average received power for an energy symbol transmitted at time t from the vehicle to the WPN is

$$P_{rx}(t) = P_{tx}^v K_0 d^{-\ell}(t), \quad (17)$$

where P_{tx}^v is the average power used by the vehicle to transmit the energy symbol and K_0 is the Friis equation parameter, ℓ is the path loss exponent and $d(t)$ is the distance from the vehicle to WPN. Note that the product $K_0 d^{-\ell}(t)$ is the square of the channel gain between the WPN and the vehicle at time t , $|\mathbf{h}(t)|^2$. Note also the dependence of the distance on time, as the vehicle is moving during the frame duration. Moreover, the Friis equation parameter can be computed as:

$$K_0 = G_v G_{\text{WPN}} \left[\frac{\lambda_{\text{WET}}}{4\pi} \right]^2, \quad (18)$$

being G_v and G_{WPN} the antenna gains of the vehicle and WPN, respectively, and λ_{WET} is the wavelength of the RF signal from the vehicle to the WPN. Note that we let the WIT stage to use another frequency band, so for that stage the Friis equation is computed using λ_{WIT} .

From the harvested power and considering that a frame starts at $t = 0$, we can easily compute the harvested energy during the WET stage as

$$E_h = \int_0^{\alpha_{\text{WET}}T} P_h(P_{rx}(t)) dt. \quad (19)$$

For the WIT stage, the required energy and time to send a packet of length L is

$$E_{\text{trx}}^{\text{WPN}} = \frac{L[P_{lc}(P_{\text{trx}}^{\text{WPN}}) + P_{\text{trx}}^{\text{WPN}}]}{R}, \quad (20)$$

$$T_{\text{trx}} = \frac{L}{R} = \alpha_{\text{WIT}}T. \quad (21)$$

being $P_{lc}(P_{\text{trx}}^{\text{WPN}})$ the power required by the circuit to send information with a power $P_{\text{trx}}^{\text{WPN}}$ and R the effective data rate selected by the WPN, which will be based on the technology and, more specifically, in its modulation and coding schemes available.

In summary, the energy consumed by a WPN for serving a vehicle during a frame is:

$$\begin{aligned} E_c &= P_{rc}^{\text{WPN}} \alpha_{\text{WET}}T + E_{\text{trx}}^{\text{WPN}} = \\ &= \left(P_{rc}^{\text{WPN}} \alpha_{\text{WET}} + P_{lc}^{\text{WPN}}(P_{\text{trx}}^{\text{WPN}}) \alpha_{\text{WIT}} \right) T, \end{aligned} \quad (22)$$

where $P_{lc}(P_{\text{trx}}^{\text{WPN}})$ accounts for the total power consumed by the WPN to transmit data with a specific power $P_{\text{trx}}^{\text{WPN}}$, with $P_{lc}(P_{\text{trx}}^{\text{WPN}}) = P_{lc}(P_{\text{trx}}^{\text{WPN}}) + P_{\text{trx}}^{\text{WPN}}$. Nevertheless, we consider a general case where the WPN stores a fraction Δ of the harvested energy to power its circuits, for example, its sensors and microcontroller, after the transmission. Therefore, the harvested energy to initiate data transmission is $(1 + \Delta)E_{\text{trx}}^{\text{WPN}}$.

V. MULTI-VEHICLE MODEL

After evaluating the bounds for transmitting data using RF-harvested energy for a single vehicle, now we focus on a multi-vehicle evaluation.

To account for multiple vehicles providing RF energy to a WPN, we must define the vehicle arrival process. We model the arrival of vehicles to the WPN using a hardcore repulsive Poisson Point Process [41]. Note that, although the randomness of the usual and mathematically tractable Poisson Point Process is desirable for modeling this setting, we cannot consider it because vehicles cannot be considered points due to their physical size. Moreover, vehicles cannot be infinitely close to each other not only due to their physical size but also due to the required safety distance between vehicles, which depends on their speed. Then, being s_m the separation of vehicles for safety and because of their length and Λ the density of vehicles expressed in vehicles per meter when safety distance is not considered, the distribution of the separation between adjacent vehicles s has been modeled as a shifted exponential distribution, being its probability density function:

$$f_s(x) \triangleq \begin{cases} \Lambda e^{-\Lambda(x-s_m)}, & \text{if } x \geq s_m \\ 0, & \text{otherwise} \end{cases}, \quad (23)$$

whose mean is $E[s] = (1 + s\Lambda)/\Lambda$. Then, the real density of vehicles including the safety distance can be computed as:

$$\Lambda_r = \frac{1}{E[s]} = \frac{\Lambda}{1 + s\Lambda}. \quad (24)$$

Then, the probability of having p vehicles in a range r_v equals to [41]:

$$\begin{aligned} P(p, r_v) &= e^{-\Lambda(r_v - ps_m)} \\ &\times \sum_{x=0}^p \frac{(\Lambda(r_v - ps_m))^x}{x!} \left(1 - \frac{\Gamma(p-x, \Lambda s_m)}{(p-x)!} \right), \end{aligned} \quad (25)$$

where $\Gamma(z, x)$ is the upper incomplete gamma function [42, Eq. 8.350.2].

Note that the above-defined repulsive hardcore Poisson Point Process can be seen as a Poisson Point Process where every distance between adjacent vehicles is increased with a safety distance, which decreases the real density of vehicles. Then, the result is a 1-dimensional Matérn hardcore point process [43], as it is guaranteed to have a minimum separation between any two points (vehicles) of the process.

On the other hand, the safety separation between adjacent vehicles for vehicle i , expressed in meters, can be modeled as:

$$s_m(i) = \max(5, v_s(i+1)/5), \quad (26)$$

with $v_s(i+1)$ being the speed of the vehicle ahead.

Additionally, we consider that the LoS between the charging vehicle and the WPN might be blocked by other vehicles. Therefore, we consider a LoS channel model for a vehicle in front of the line and, for the rest of vehicles, we introduce a non-zero probability of communicating in a non-line of sight (NLoS) channel model, which is an increasing function of the density of vehicles. We adopt the NLoS channel model described in [44].

Note that, in a multivehicle setting, the RF EH signals transmitted by different vehicles may arrive at the WPN with different phases, resulting in a sub-optimal amount of harvested energy. To mitigate this problem, EH nodes with multiple antennas can employ phase shifters to synchronize the phase of the incoming signals [45], [46]. However, the design of EH solutions that involve the use of phase shifters is out of the scope of this paper since we consider a single-antenna WPN. Instead, our analyses in the multivehicle scenario focus on the upper bound of performance, which is achieved when the phases of the incoming EH signals are synchronized. Such synchronization can be achieved, for example, using V2V communication to synchronize the phases of the signals from the vehicles in a platoon so that these operate as distributed MIMO arrays [47].

VI. PERFORMANCE EVALUATION

The performance evaluation of the proposal is done in three steps. First, we analyze the WET stage when the vehicle is driving near the WPN. Second, we make an in-depth analysis of the feasibility of the whole procedure

TABLE 3. Summary of the parameter settings for performance evaluation.

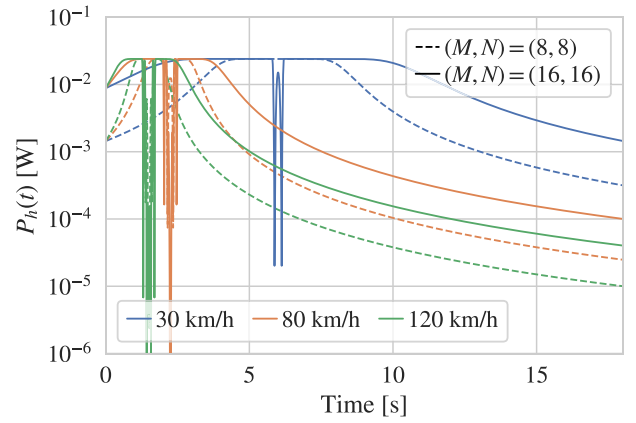
Parameter	Symbol	Value
Vehicle speed [km/h]	v_s	[30, 120]
Maximum harvested power [mW]	P_h^{\max}	24
Vehicle transmission power [dBm]	P_{tx}^v	36
Frequency band for WET [MHz]	f_{WET}	434
Path loss exponent	ℓ	2
Minimum vehicle-to-WPN distance [m]	r	3
Size of the URPA	(M, N)	$\{(8, 8), (16, 16)\}$
Quality of the beam tracking	ξ	4
WPN transmission power [dBm]	P_{tx}^{WPN}	23
Power consumed to transmit [mW]	P_{tc}	716
Noise power density [dB/Hz]	N_0	-136
Data transmission rate [kbit/s]	R	120
Frequency band for WIT [MHz]	f_{WIT}	800
Bandwidth for WIT [kHz]	B	180

including both WET and WIT stages. Third, we evaluate a setting including both WET and WIT stages including multiple vehicles. Note that a summary of the default parameter settings considered for evaluation is provided in Table 3.

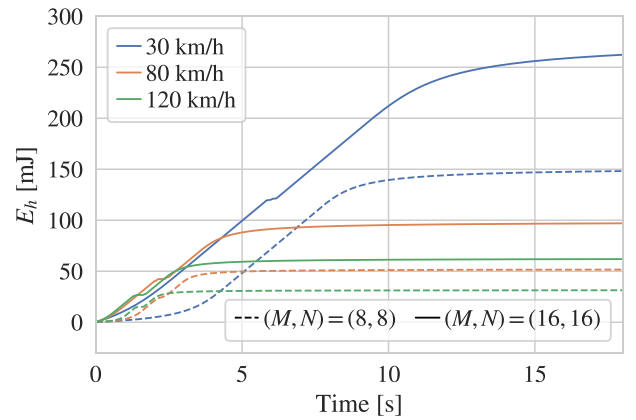
A. ENERGY HARVESTING

In this section, we evaluate how can be energy harvested in a WPN when a vehicle drives nearby to it and study how it changes according to the vehicle's speed. Concerning the parameters used for the evaluation, all of them have been accurately configured following real measurements or feasible configurations. For the parameters that define the energy harvesting model, we have considered the values that fit experimental measures proposed in [34], being $\sigma = 1500$, $\zeta = 0.0014$ and the maximum reachable harvested power $P_h^{\max} = 24$ mW. Note that these values have been widely used [19], [21]. The WPN is equipped with an isotropic antenna, which allows it to receive energy and data from multiple directions with minimal complexity. On the other hand, and regarding the URPA at the vehicle, we have considered two antenna sizes: $(M, N) = (8, 8)$ and $(M, N) = (16, 16)$. As seen in Fig. 3, the latter results in a higher gain but also a higher sensitivity to beam alignment errors than the former. To account for the quality of the beam tracking technique, we set ξ (see Section IV) to a pessimistic value of $\xi = 4$. With this value, the maximum beam alignment error is 31.3° , occurring at the maximum vehicle speed under consideration ($v_s = 120$ km/h). For the lowest speed under consideration ($v_s = 30$ km/h) the maximum BTE is slightly lower than 9° . Note that the maximum BTE is obtained for the highest angular velocity of the vehicle, which occurs when the vehicle is close to the WPN.

In Fig. 4, we show the harvested power and the accumulated harvested energy at the WPN when a vehicle, with



(a) Harvested power.



(b) Harvested energy.

FIGURE 4. Harvested power and energy for different vehicle speeds and URPA sizes.

different speeds, drives nearby and for two different antenna sizes (8×8 and 16×16). As expected, when the vehicle speed is lower the harvesting stage takes for a longer time so it is possible to saturate the EH circuitry for a longer time. Additionally, the amount of harvested energy that the WPN can collect for different vehicle speeds decreases with the vehicle's speed. If we evaluate Fig. 4a in detail, we find that the higher directivity of the 16×16 antenna array allows us to expand the time where the energy is being harvested. Furthermore, we observe some sudden falls in the harvested power when the beam alignment is out of the main lobe. This behavior, as expected, occurs when the vehicle is close to the WPN because its angular velocity is higher and is more severe for the 16×16 array, as its beamwidth is lower. Notwithstanding, and according to Fig. 4b, more energy can be harvested with the 16×16 array than with the 8×8 array, so, from the rest of experiments, we consider a 16×16 URPA for the vehicle.

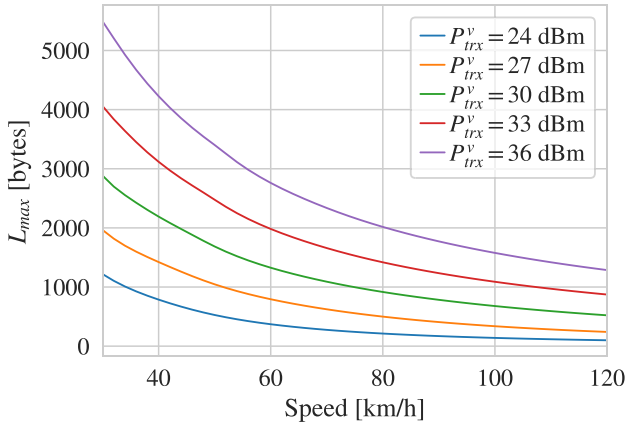


FIGURE 5. Maximum data that the WPN can transmit as a function of the vehicle speed.

B. DATA TRANSMISSION CAPACITY

After an evaluation of the EH procedure to ease its understanding, now we study the feasibility and capacity of the WPN to be able to transmit data using only the harvested energy. For the parameters related to data transmission, we choose realistic values inspired by those used in the 3GPP NB-IoT technology. For example, we consider that a QPSK modulation together with a 1/3 coding scheme are used. Then, for the selected bandwidth of $B = 180$ kHz, we obtain $R = 120$ kbit/s. Additionally, we consider that, among the available set of transmission powers for NB-IoT, we choose $P_{tx}^{WPN} = 23$ dBm. For the power consumption required to send data, we resort to the measurements presented in [48], so to send data with a transmission power of 23 dBm, the chipset requires $P_{lc} = 716$ mW. Similar measurements that confirm the accuracy of the chosen proposal can be found in [49], [50] and also in the specifications of the NB-IoT module u-blox SARA-N2, with a maximum consumption of 220 mA at 3.6 V in transmission mode. Finally, we consider a noise density power of $N_0 = -136$ dB.

First, we study the maximum capacity of the WPN to send data with the harvested energy. In a nutshell, we study the maximum data size that can be sent by the WPN using the energy harvested from the RF signal transmitted by the vehicle. Note that this data can be either encrypted or not and also can include a hash to verify its integrity at the receiver but we do not focus on the computation effort of the cypher and hashing as this information can be precomputed in the WPN. In Fig. 5, we show the maximum data that can be sent by the WPN to the vehicle as a function of the speed of the vehicle and for different transmission powers for EH. A first conclusion is that it is feasible to send data with the harvested energy, especially at low speeds, where we can send more than 5 kbytes of data. Moreover, and as expected, the amount of data that can be sent increases as the transmission power of the vehicle to charge the roadside node increases. Notwithstanding, for low transmission powers like $P_{tx}^v = 24$ dBm, we can send more than to 1 kbyte of data.

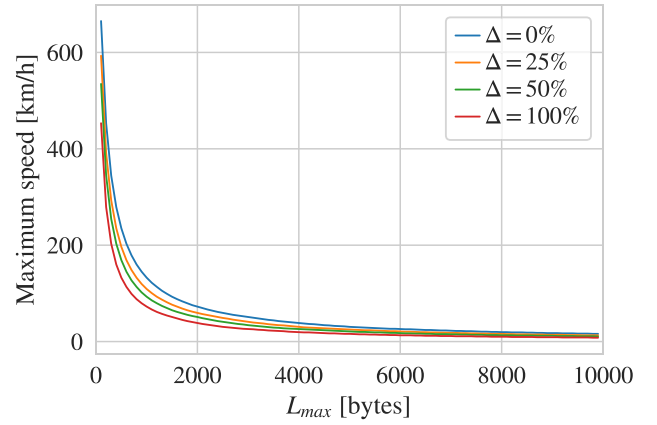


FIGURE 6. Maximum speed of the vehicle to send L_{max} bytes.

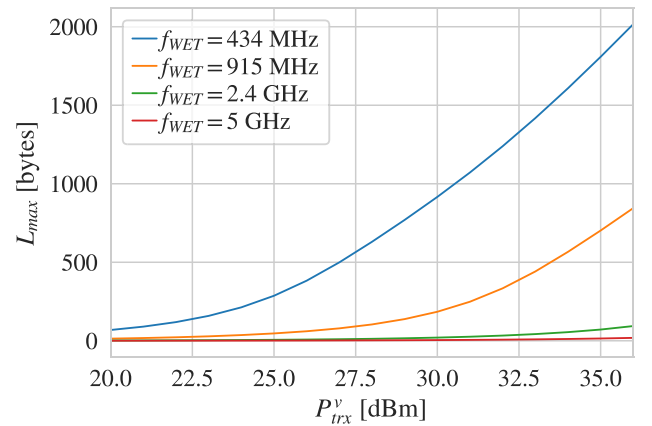


FIGURE 7. Maximum data that the WPN can transmit as a function of the transmit power for different frequency bands for EH.

Now we study the inverse problem, i.e., the maximum speed that a vehicle can drive to be able to send packets of a certain size. These results are shown in Fig. 6. In this figure we also consider the case when the WPN needs additional energy to power, for example, some sensors whose measurements are used in the data sent. This energy, additional to the energy required to transmit data, is defined by Δ , as defined in Section IV. As an example, when $\Delta = 50\%$, we refer to the situation when we must harvest 50% more energy than the needed for data transmission. Results show that the maximum speed that a vehicle can have to be able to send data rapidly decreases with the size of that data. Moreover, as we need more additional energy for powering other circuits of the WPN, the maximum speed of the vehicle decreases.

One of the decisions to make for harvesting energy is about the frequency band to use. In this work, we have focused on the use of unlicensed ISM bands for the WET stage. In Fig. 7, we show the impact of the choice of the frequency band for sending RF charging signals and conclude that lower frequencies are preferable to harvest more energy. Of course, this choice will be guided by external factors like other wireless services that can be interfered with or

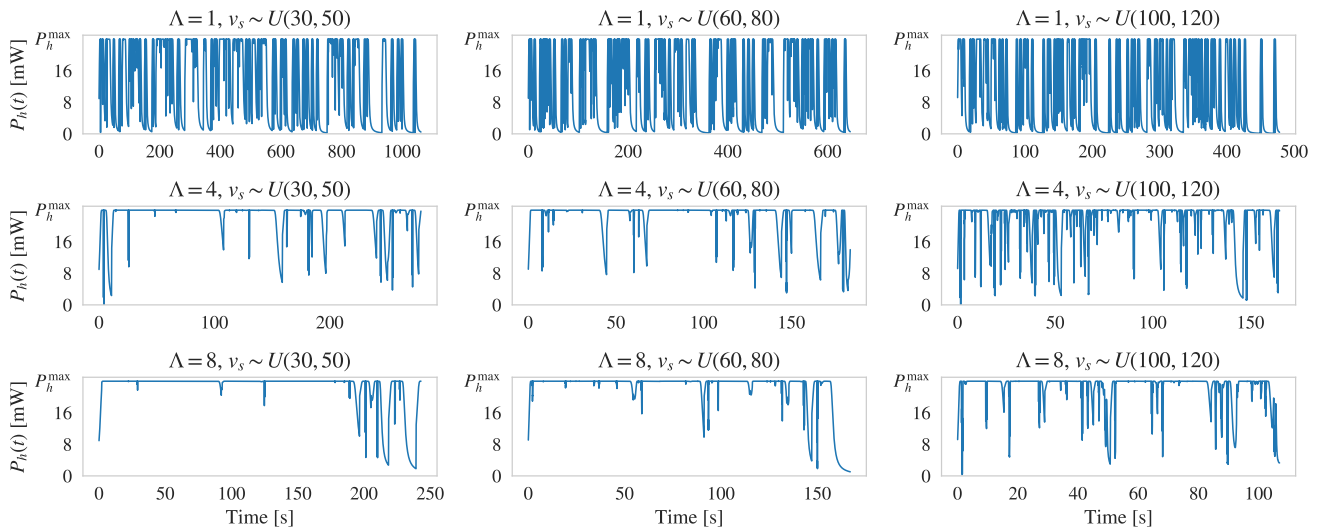


FIGURE 8. Harvested power in multi-vehicle setting for urban (left), rural (center), and highway (right) scenarios.

even the specific world region, as unlicensed bands vary. Results show that the frequency band with the best capacity to harvest energy is the lowest band. Moreover, results also show that both 2.4 and 5 GHz frequency bands are not useful for our purpose.

C. MULTI-VEHICLE EVALUATION

The evaluation of the multi-vehicle setting is performed in two steps. First, we evaluate how the WPN can harvest energy when multiple vehicles pass by. Second, we analyze the capacity of the WPN for sending data using the harvested energy. In Fig. 8, we show the harvested power for different densities of vehicles (Λ , expressed in vehicles per 100 meters) and for different speeds. For the speeds, we have considered three types of roads: i) urban, where we have considered that the speed of vehicles is uniformly distributed with a minimum and maximum of 30 and 50 km/h ($U(30,50)$), ii) interurban roads, where the speed of vehicles is $U(60,80)$, and iii) motorways, where the speed of vehicles is $U(100,120)$. For the NLoS channel model for those settings, we have considered the urban, rural, and highway settings defined in [44], with path loss exponents 2.25, 2.34, and 2.98, respectively. Moreover, we have considered three densities: $\Lambda \in \{1, 5, 8\}$ vehicles per 100 meters, to represent situations of light, medium, and dense traffic. Note that for all these three densities we have considered the probability of NLoS (P_{NLoS}) to be 0, 0.2, and 0.4, respectively. Moreover, all the results shown in Fig. 8 considered a total of 100 vehicles. Results show that when density Λ increases and speed decreases, the amount of time when the WPN EH circuitry is saturated increases, so the capacity of harvesting energy decreases.

On the other hand, in Table 4 we show the maximum amount of data (measured in bytes) that can be sent to each vehicle using the harvested energy. Note that the values have been obtained considering 1000 vehicles. Moreover,

TABLE 4. Maximum packet size in bytes per vehicle that can be transmitted using harvested energy.

	Speed		
	40	70	110
Single vehicle	4243	2304	1392

	Λ	Speed range		
		U(30, 50)	U(60, 80)	U(100, 120)
Multivehicle	1	2991	1799	1066
	4	1277	935	661
	8	1078	676	495

for comparison purposes, we also include the results for the single-vehicle setting. As it can be seen, when the density Λ increases the transmission capacity of data decreases due to the saturation of the EH circuitry, as shown in Fig. 8.

VII. CONCLUSION

Future ITS will radically change human mobility. Notwithstanding, complex services such as autonomous driving require the deployment and operation of a huge number of communication devices across the transportation infrastructure. Providing energy to such a large number of roadside network devices, either using batteries or a connection to the power grid, is costly, especially in long highways or rural areas. To mitigate the costs related to the energy supply of these devices, we evaluated in this paper the limits on the communication of data when roadside network nodes are powered by passing vehicles using RF EH. Results showed that it is possible to send small amounts of data using only the harvested energy from passing vehicles. Moreover, we analyzed the different factors that limit the amount of data that roadside nodes can transmit. Future work includes a feasibility analysis with intelligent roadside nodes, which use the harvested energy not only for communication

purposes but also for small computation tasks, enriching the possibilities of V2I communications.

REFERENCES

- [1] A. Gohar and G. Nencioni, "The role of 5G technologies in a smart city: The case for intelligent transportation system," *Sustainability*, vol. 13, no. 9, p. 5188, 2021.
- [2] M. Parvini, P. Schulz, and G. Fettweis, "Resource allocation in V2X networks: From classical optimization to machine learning-based solutions," *IEEE Open J. Commun. Soc.*, vol. 5, pp. 1958–1974, 2024.
- [3] M. A. Hassan et al., "Intelligent transportation systems in smart city: A systematic survey," in *Proc. Int. Conf. Robot. Autom. Ind. (ICRAI)*, 2023, pp. 1–9.
- [4] A. Imghoure, F. Omary, and A. El-Yahyaoui, "Schnorr-based conditional privacy-preserving authentication scheme with multisignature and batch verification in VANET," *Internet Things*, vol. 23, Oct. 2023, Art. no. 100850.
- [5] O. M. Rosabal, O. L. A. López, H. Alves, and M. Latva-Aho, "Sustainable RF wireless energy transfer for massive IoT: Enablers and challenges," *IEEE Access*, vol. 11, pp. 133979–133992, 2023.
- [6] S. Goyal, N. Sharma, I. Kaushik, B. Bhushan, and N. Kumar, "A green 6G network era: Architecture and propitious technologies," in *Proc. Data Anal. Manag. (ICDAM)*, 2021, pp. 59–75.
- [7] H. Elahi, K. Munir, M. Eugeni, S. Atek, and P. Gaudenzi, "Energy harvesting towards self-powered IoT devices," *Energies*, vol. 13, no. 21, p. 5528, 2020.
- [8] O. L. Alcaraz López et al., "Massive wireless energy transfer: Enabling sustainable IoT toward 6G era," *IEEE Internet Things J.*, vol. 8, no. 11, pp. 8816–8835, Jun. 2021.
- [9] Z. Lv and W. Shang, "Impacts of intelligent transportation systems on energy conservation and emission reduction of transport systems: A comprehensive review," *Green Technol. Sustain.*, vol. 1, no. 1, 2023, Art. no. 100002.
- [10] J. Wang, K. Zhu, and E. Hossain, "Green Internet of Vehicles (IoV) in the 6G era: Toward sustainable vehicular communications and networking," *IEEE Trans. Green Commun. Netw.*, vol. 6, no. 1, pp. 391–423, Mar. 2022.
- [11] A. Muhtar, B. R. Qazi, S. Bhattacharya, and J. M. Elmirghani, "Greening vehicular networks with standalone wind powered RSUs: A performance case study," in *Proc. IEEE Int. Conf. Commun. (ICC)*, 2013, pp. 4437–4442.
- [12] R. Atallah, M. Khabbaz, and C. Assi, "Energy harvesting in vehicular networks: A contemporary survey," *IEEE Wireless Commun.*, vol. 23, no. 2, pp. 70–77, Apr. 2016.
- [13] Q. I. Ali, "Green communication infrastructure for vehicular ad hoc network (VANET)," *J. Elect. Eng.*, vol. 16, no. 2, pp. 1–10, 2016.
- [14] F. Han, A. W. Bandarkar, and Y. Sozer, "Energy harvesting from moving vehicles on highways," in *Proc. IEEE Energy Convers. Congr. Expo. (ECCE)*, 2019, pp. 974–978.
- [15] D. Altinel and G. K. Kurt, "Modeling of multiple energy sources for hybrid energy harvesting IoT systems," *IEEE Internet Things J.*, vol. 6, no. 6, pp. 10846–10854, Dec. 2019.
- [16] X. Wang et al., "Future communications and energy management in the Internet of Vehicles: Toward intelligent energy-harvesting," *IEEE Wireless Commun.*, vol. 26, no. 6, pp. 87–93, Dec. 2019.
- [17] H. Xiao et al., "Energy-efficient resource allocation in radio-frequency-powered cognitive radio network for connected vehicles," *IEEE Trans. Intell. Transp. Syst.*, vol. 22, no. 8, pp. 5426–5436, Aug. 2021.
- [18] Z. Yang, W. Xu, and M. Shikh-Bahaei, "Energy efficient UAV communication with energy harvesting," *IEEE Trans. Veh. Technol.*, vol. 69, no. 2, pp. 1913–1927, Feb. 2020.
- [19] Q.-V. Pham, M. Le, T. Huynh-The, Z. Han, and W.-J. Hwang, "Energy-efficient federated learning over UAV-enabled wireless powered communications," *IEEE Trans. Veh. Technol.*, vol. 71, no. 5, pp. 4977–4990, May 2022.
- [20] Q. Wu, W. Chen, D. W. K. Ng, J. Li, and R. Schober, "User-centric energy efficiency maximization for wireless powered communications," *IEEE Trans. Wireless Commun.*, vol. 15, no. 10, pp. 6898–6912, Oct. 2016.
- [21] T.-T. Nguyen, V.-D. Nguyen, Q.-V. Pham, J.-H. Lee, and Y.-H. Kim, "Resource allocation for AF relaying wireless-powered networks with nonlinear energy harvester," *IEEE Commun. Lett.*, vol. 25, no. 1, pp. 229–233, Jan. 2021.
- [22] T. A. Khan, A. Yazdan, and R. W. Heath, "Optimization of power transfer efficiency and energy efficiency for wireless-powered systems with massive MIMO," *IEEE Trans. Wireless Commun.*, vol. 17, no. 11, pp. 7159–7172, Nov. 2018.
- [23] F. Wang, J. Xu, X. Wang, and S. Cui, "Joint offloading and computing optimization in wireless powered mobile-edge computing systems," *IEEE Trans. Wireless Commun.*, vol. 17, no. 3, pp. 1784–1797, Mar. 2018.
- [24] S. Bi and Y. J. Zhang, "Computation rate maximization for wireless powered mobile-edge computing with binary computation offloading," *IEEE Trans. Wireless Commun.*, vol. 17, no. 6, pp. 4177–4190, Jun. 2018.
- [25] F. Zhou and R. Q. Hu, "Computation efficiency maximization in wireless-powered mobile edge computing networks," *IEEE Trans. Wireless Commun.*, vol. 19, no. 5, pp. 3170–3184, May 2020.
- [26] H. Shi, R. Luo, and G. Gui, "Joint offloading and energy optimization for wireless powered mobile edge computing under nonlinear eh model," *Peer-to-Peer Netw. Appl.*, vol. 14, no. 4, pp. 2248–2261, 2021.
- [27] Y. Song, Y. Xiao, Y. Chen, G. Li, and J. Liu, "Deep reinforcement learning enabled energy-efficient resource allocation in energy harvesting aided V2X communication," in *Proc. IEEE 33rd Annu. Int. Symp. Pers., Indoor Mobile Radio Commun. (PIMRC)*, 2022, pp. 313–319.
- [28] H. Alves and O. A. Lopez, *Wireless RF Energy Transfer in the Massive IoT Era: Towards Sustainable Zero-energy Networks*. Hoboken, NJ, USA: IEEE Press, Wiley, 2022.
- [29] H. Zeb et al., "Zero energy IoT devices in smart cities using RF energy harvesting," *Electronics*, vol. 12, no. 1, p. 148, 2022.
- [30] M. Cansiz and D. Altinel, "Multiband RF energy harvesting for zero-energy devices," *Elect. Eng.*, vol. 105, no. 1, pp. 91–100, 2023.
- [31] F. Librino and P. Santi, "EH from V2X communications: The price of uncertainty and the impact of platooning," *IEEE Trans. Veh. Technol.*, vol. 73, no. 1, pp. 385–401, Jan. 2024.
- [32] T. D. P. Perera, D. N. K. Jayakody, S. K. Sharma, S. Chatzinotas, and J. Li, "Simultaneous wireless information and power transfer (SWIPT): Recent advances and future challenges," *IEEE Commun. Surveys Tuts.*, vol. 20, no. 1, pp. 264–302, 1st Quart., 2018.
- [33] E. Boshkovska, D. W. K. Ng, N. Zlatanov, and R. Schober, "Practical non-linear energy harvesting model and resource allocation for SWIPT systems," *IEEE Commun. Lett.*, vol. 19, no. 12, pp. 2082–2085, Dec. 2015.
- [34] E. Boshkovska, R. Morsi, D. W. K. Ng, and R. Schober, "Power allocation and scheduling for SWIPT systems with non-linear energy harvesting model," in *Proc. IEEE Int. Conf. Commun. (ICC)*, 2016, pp. 1–6.
- [35] D.-W. Lim, C.-J. Chun, and J.-M. Kang, "Transmit power adaptation for D2D communications underlying SWIPT-based IoT cellular networks," *IEEE Internet Things J.*, vol. 10, no. 2, pp. 987–1000, Jan. 2023.
- [36] S. Li, J. Zhao, W. Tan, and C. You, "Optimal secure transmit design for wireless information and power transfer in V2X vehicular communication systems," *AEU-Int. J. Electron. Commun.*, vol. 118, May 2020, Art. no. 153148.
- [37] H. Ju and R. Zhang, "Throughput maximization in wireless powered communication networks," *IEEE Trans. Wireless Commun.*, vol. 13, no. 1, pp. 418–428, Jan. 2014.
- [38] C. A. Balanis, *Antenna Theory: Analysis and Design*. Hoboken, NJ, USA: Wiley, 2016.
- [39] T. Lo, "Maximum ratio transmission," *IEEE Trans. Commun.*, vol. 47, no. 10, pp. 1458–1461, Oct. 1999.
- [40] C. Liu et al., "Robust adaptive beam tracking for mobile millimetre wave communications," *IEEE Trans. Wireless Commun.*, vol. 20, no. 3, pp. 1918–1934, Mar. 2021.
- [41] H. Nguyen et al., "Impact of big vehicle shadowing on vehicle-to-vehicle communications," *IEEE Trans. Veh. Technol.*, vol. 69, no. 7, pp. 6902–6915, Jul. 2020.
- [42] I. S. Gradshteyn and I. M. Ryzhik, *Table of Integrals, Series, and Products*. Waltham, MA, USA: Acad. Press, 2014.
- [43] F. Baccelli and P. Berman, "Extremal versus additive matérn point processes," *Queueing Syst.*, vol. 71, pp. 179–197, Jun. 2012.

- [44] H. Fernández, L. Rubio, V. M. Rodrigo-Peñarocha, and J. Reig, "Path loss characterization for vehicular communications at 700 MHz and 5.9 GHz under LOS and NLOS conditions," *IEEE Antennas Wireless Propag. Lett.*, vol. 13, pp. 931–934, 2014.
- [45] O. L. López, B. Clerckx, and M. Latva-Aho, "Dynamic RF combining for multi-antenna ambient energy harvesting," *IEEE Wireless Commun. Lett.*, vol. 11, no. 3, pp. 493–497, Mar. 2022.
- [46] S. Arzykulov, G. Naurzybayev, A. Celik, and A. M. Eltawil, "RIS-assisted full-duplex relay systems," *IEEE Syst. J.*, vol. 16, no. 4, pp. 5729–5740, Dec. 2022.
- [47] Z. Huang, L. Bai, M. Sun, and X. Cheng, "A 3D non-stationarity and consistency model for cooperative multi-vehicle channels," *IEEE Trans. Veh. Technol.*, vol. 72, no. 9, pp. 11095–11110, Sep. 2023.
- [48] M. Lauridsen, R. Krigslund, M. Rohr, and G. Madueno, "An empirical NB-IoT power consumption model for battery lifetime estimation," in *Proc. IEEE 87th Veh. Technol. Conf. (VTC Spring)*, 2018, pp. 1–5.
- [49] P. Andres-Maldonado, M. Lauridsen, P. Ameigeiras, and J. M. Lopez-Soler, "Analytical modeling and experimental validation of NB-IoT device energy consumption," *IEEE Internet Things J.*, vol. 6, no. 3, pp. 5691–5701, Jun. 2019.
- [50] R. Marini, K. Mikhaylov, G. Pasolini, and C. Buratti, "Low-power wide-area networks: Comparison of LoRaWAN and NB-IoT performance," *IEEE Internet Things J.*, vol. 9, no. 21, pp. 21051–21063, Nov. 2022.



JOSE MANUEL GIMENEZ-GUZMAN received the M.S. and Ph.D. degrees (cum laude and extraordinary prize) in telecommunication engineering from the Universitat Politècnica de València, Spain, in 2002 and 2008, respectively. From 2008 to 2021, he was an Associate Professor with the University of Alcalá, Spain. He is currently an Associate Professor with the Universitat Politècnica de València, where he is engaged in research and teaching in the areas of analysis and performance evaluation of wireless networks and optimization of complex networked systems. He has been a Visiting Scholar with the University of Würzburg, Germany, and with Aalborg University, Denmark, in 2012 and 2023, respectively. He has published more than 60 technical papers in these areas in international journals and conference proceedings. He is also an Associate Editor of the *Wireless Networks*.



ISRAEL LEYVA-MAYORGA (Member, IEEE) received the B.Sc. degree in telematics engineering and the M.Sc. degree (Hons.) in mobile computing systems from the Instituto Politécnico Nacional, Mexico, in 2012 and 2014, respectively, and the Ph.D. degree (cum laude and extraordinary prize) in telecommunications from the Universitat Politècnica de València (UPV), Spain, in 2018. He was a Visiting Researcher with the Department of Communications, UPV in 2014, and with the Deutsche Telekom Chair of Communication Networks, Technische Universität Dresden, Germany, in 2018. He is currently an Assistant Professor with the Connectivity Section (CNT), Department of Electronic Systems, Aalborg University, Denmark, where he served as a Postdoctoral Researcher from January 2019 to July 2021. His research interests include beyond-5G, and 6G networks, satellite communications, and random and multiple access protocols. He is an Associate Editor for IEEE WIRELESS COMMUNICATIONS LETTERS, and a Board Member of one6G.



AMIRHOSSEIN AZARBAHRAM (Graduate Student Member, IEEE) received the B.Sc. degree in telecommunications from the KN Toosi University of Technology, Iran, in 2020, and the M.Sc. degree in communications system from the Sharif University of Technology, Iran, in 2022. He is currently a Doctoral Researcher with the Centre for Wireless Communications, University of Oulu, Finland. He was a Visiting Researcher with the Connectivity Section (CNT), Department of Electronic Systems, Aalborg University, Denmark, in 2024. His research interests include wireless communications and RF wireless power transfer.



ONEL ALCARAZ LÓPEZ (Senior Member, IEEE) received the B.Sc. degree (First-Class Hons.) from the Central University of Las Villas, Cuba, in 2013, the M.Sc. degree from the Federal University of Paraná, Brazil, in 2017, and the D.Sc. degree (with Distinction) in electrical engineering from the University of Oulu, Finland, in 2020, where he currently holds an Associate Professorship (tenure track) of Sustainable Wireless Communications Engineering with the Centre for Wireless Communications. He is a Co-Author of the books titled *Wireless RF Energy Transfer in the Massive IoT Era: Toward Sustainable Zero-Energy Networks* (Wiley, 2021), and *Ultra-Reliable Low-Latency Communications: Foundations, Enablers, System Design, and Evolution Towards 6G* (Now Publishers, 2023). His research interests include wireless communications, signal processing, sustainable IoT, and wireless RF energy transfer. He is a collaborator to the 2016 Research Award given by the Cuban Academy of Sciences, a co-recipient of the 2019 and 2023 IEEE EuCNC Best Student Paper Award, and the recipient of the 2020 Best Doctoral Thesis Award granted by Finland TEK and TFiF and the 2022 Young Researcher Award in the field of technology in Finland.



PETAR POPOVSKI (Fellow, IEEE) received the Dipl.-Ing and M.Sc. degrees in communication engineering from the University of Sts. Cyril and Methodius in Skopje, and the Ph.D. degree from Aalborg University in 2005. He is a Professor with Aalborg University, where he heads the section on Connectivity, and a Visiting Excellence Chair with the University of Bremen. He authored the book *Wireless Connectivity: An Intuitive and Fundamental Guide*. His research interests are in the area of wireless communication and communication theory. He received an ERC Consolidator Grant in 2015, the Danish Elite Researcher Award in 2016, the IEEE Fred W. Ellersick Prize in 2016, the IEEE Stephen O. Rice Prize in 2018, the Technical Achievement Award from the IEEE Technical Committee on Smart Grid Communications in 2019, the Danish Telecommunication Prize in 2020, and the Villum Investigator Grant in 2021. He is currently the Editor-in-Chief of IEEE JOURNAL ON SELECTED AREAS IN COMMUNICATIONS and the Chair of the IEEE Communication Theory Technical Committee. He was a Member-at-Large at the Board of Governors in IEEE Communication Society from 2019 to 2021. He was the General Chair for IEEE SmartGridComm 2018 and IEEE Communication Theory Workshop 2019.